Atomic force microscopy

M12. Pablo Hernández López, Lucía Navarro

December 2018

1 Introduction

The aim of this experiment is to become familiar with the working principle of the Atomic Force Microscope, as we will use it to determine the surface topography of two different samples and study the effects of electrostatic potentials.

2 Theory

2.1 The atomic force microscope

The most common examples of Scanning Probe Microscopes (SPM, a family of instruments for studying surfaces at an atomic level) are the Scanning Tunneling Microscope (STM) and the Atomic Force Microscope (AFM).

The Scanning Tunneling Microscope uses the quantum mechanical tunnel effect to map the surface of conductive samples. There is a fine metal tip which has been sharpened to the atomic level and is held in a potential difference with the sample that will be studied. It is moved above the surface so for a certain separation distance, the tunnel effect occurs and a current is generated in the conductive material. Being the tunneling current exponentially proportional to the distance between tip and sample, the STM gives us a very accurate picture of the sample surface's topography.

The Atomic Force Microscope was invented later, motivated by the fact that the STM only works for conductive samples and the AFM can be used in any material. In this microscope a fine tip is placed at the free end of a cantilever, and here it will be the atomic force between the tip and the sample who will give us information about the surface topography. When the tip gets close enough to the sample, the variation of the forces between them will make the cantilever bend. A detector measures the deflections of the cantilever as the sample is scanned and these measures allow a computer to generate a map of the surface topography. The AFM consists thus of a cantilever and a small tip at the end, a laser, a 4-quadrant photodiode and a scanner, as shown in Figure 1.

Atomic Force Microscopes can be operated in two different modes: the contact mode, where the tip scans the surface at less than a few angstroms of distance to the sample and the interaction force with it is repulsive, and the non-contact mode (NC-AFM), where the distance to the sample ranges from the tens to the thousands of angstroms and the interaction force is attractive.

2.2 Contact AFM

In the contact mode of the AFM the tip is in the regime of distances where the Lennard-Jones potential, the main force between tip and sample, is positive and thus the force is repulsive. This is due to the Pauli's exclusion force between the overlapping clouds of electrons and also their electrostatic repulsion as distributions of charge of the same sign. In addition to these Lennard-Jones forces a capillary force with the layer of water covering the sample (in a non-vacuum situation) and the force exerted by the cantilever itself must be considered. The tip of the AFM then makes "soft physical contact" with the sample and scans it, the cantilever where the tip is attached being deflected by the forces of the different features that we may encounter in the surface. The data of this deflection may be translated to topographic data in two ways: the constant height mode or the constant force one.

2.3 Non-contact AFM

In the non-contact mode the cantilever oscillates very near to its resonance frequency while being held at distances form the sample that range from the tens to the thousands of angstroms. Here is not directly the deflection of the cantilever which give us the information about the topography of the surface but the changes in the frequency or amplitude of its oscillating motion, which are affected by the changes in the force between tip and sample. This total force is in this mode generally very low, what makes it suited for the study of soft or elastic samples. Moreover the sample is not contaminated through contact with the tip, being this another advantage of this mode.

The parameters of the vibration of the cantilever, frequency and amplitude, range from 10-100 kHz and from ten to the thousands of angstroms, respectively. The change of the resonant frequency while scanning relates to the tip-sample separation in the following way: the resonant frequency depends on the square root of the spring constant of the oscillation, which at the same time depends on the force gradient experience by the cantilever which is directly proportional to the tip-sample separation. In this mode the parameters of the vibration are kept constant through, again, a feedback circuit and it is the motion of the scanner what is used to generate the data set. It can also be operated in the two modes that will be described in the following: the constant height mode and the constant force one.

2.4 Scanning modes

At the constant height mode the distance from the tip to the sample remains the same during the scanner and it is the deflection of the cantilever which is directly interpreted as the topographic data. On the other hand, in the constant force mode it is the force between tip and sample which it is maintained constant with a feedback circuit which takes the input of the deflection of the cantilever information and controls the motion of the scanner where the sample is placed. It will be precisely this motion which will be read as the topographic data. Even if the speed of the constant force mode is limited by the time response of the feedback circuit it is normally preferred as an operation mode because it allow us to control the force exerted on the sample. These two scanning modes can be used in contact and non-contact Atomic Force Microscopy.

2.5 Atomic forces between tip and sample

The atomic forces between the tip and the sample, the main physical quantity that allow us to map the surface, can be divided in the four following categories:

$$F_{total} = F_{chemical} + F_{VdW} + F_{electrostatic} + F_{magnetic} \tag{1}$$

- $F_{magnetic}$ will not be relevant for our experiment.
- $F_{chemical}$ consists basically in the short-ranged chemical interactions described in the Lennard-Jones potential, already mentioned in section 2.2, for it divides the two regimes of distances: contact and non-contact. The shape of this potential is represented in Figure 1 and mathematically expressed in Equation 2:

$$U_{L-J} = 4\epsilon \left[\left(\frac{\sigma_0}{r} \right)^{12} - \left(\frac{\sigma_0}{r} \right)^{6} \right] \tag{2}$$

  Where the quantities ϵ and σ_0 describe the amplitude of the potential and the distance where the potential is zero, respectively.

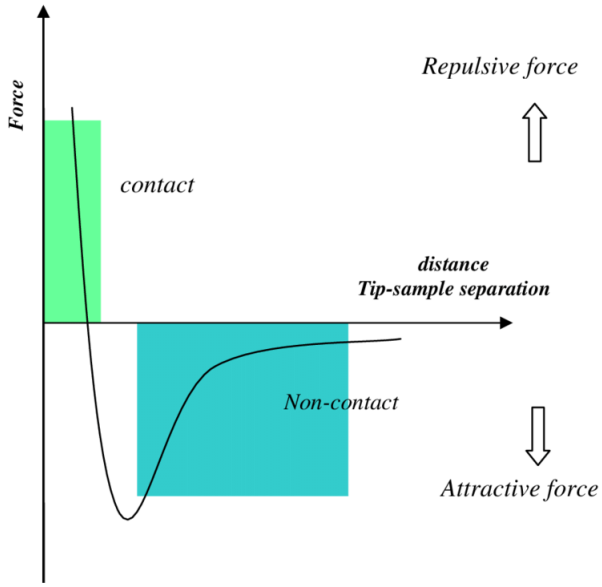

Figure 1. Representation of a Lennard-Jones potential depending on the distance r. We can see that for small distances (contact mode) the force between tip and sample is repulsive and for larger distances (non-contact mode) it starts to be attractive but less intense as r grows.

- $F_{VanderWaals}$ is due to the interaction between permanent and temporary dipoles. Permanent dipoles are those in the molecules that due to the difference of electronegativity of their atoms have an asymmetric distribution of charge; temporary dipoles are those that arise in neutral molecules due to random fluctuation of their distribution of charge. Considering our tip a sphere we can approximate this interaction as

$$F_{VdW} = \frac{HR}{6d^2} \tag{3}$$

where in this case H is the Hamecker constant, R the radius of the tip and d the tip-sample distance.

- Finally, $F_{electrostatic}$ is a result of the fact that the tip and the sample form a capacitor of capacitance C. Then this force can be written as

$$F_{elec} = \frac{1}{2}\frac{\partial C}{\partial z}V_{eff}^2 \tag{4}$$

Where V_{eff} is the total applied voltage, this is the sum of the applied voltage from the outside and the contact potential, which is due to the difference of work functions of the sample and the tip. We shall measure this last magnitude through spectroscopy.

As a result of this total force the cantilever will describe the motion of a damped harmonic oscillator with forced oscillation (non-contact mode). The interaction between the tip and the sample, this is, the changes in this total force F_{total} will change the spring constant and if this changes are small enough (smaller than the oscillation amplitude) the resulting variation of the resonance frequency ω_0 will be that of the following equation

$$\Delta\omega_0 = -\frac{\omega_0}{2k}\frac{\partial F_{total}}{\partial z} \tag{5}$$

where k is the spring constant of the cantilever. We can as well derive the force gradient from a change in the amplitude of the oscillations:

$$\frac{\partial F_{total}}{\partial z} = k\frac{1 - 2a^2 + \sqrt{4Q^2(a^2-1)+1}}{2(Q^2 - a^2)} \tag{6}$$

where a is the ratio of the free amplitude of oscillation and the amplitude of regulation and Q, the quality factor of the cantilever.

3 Instruments and procedure

The setup that will be used in this experiment is schematically shown in Figure 2. The microscope that we are going to use is provided by Nanotec. It will consist on a scanner, the piezoelectric element, and the AFM head (laser generator, photodiode and cantilever with sharpened tip). We will also need a computer with the software WSxM 4.0 Develop 8.x to see the images that will be created. Some comments on the detector, the scanner and the tip are made following.

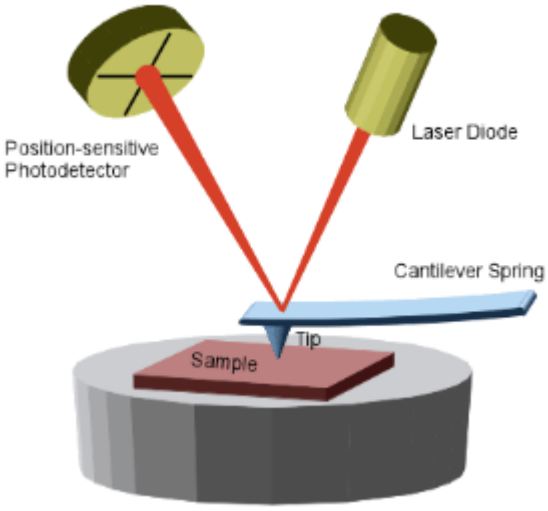

Figure 2. Schematic drawing of the experimental setup for the AFM head. The force between tip and sample will produce a variation in the bending of the cantilever, which can be detected with a laser reflecting on the cantilever to a position-sensitive photodiode.

The deflection of the cantilever will be measured through a position-sensitive photodetector with four cells that can measure the displacement of the light of the laser beam reflected at the cantilever of tens of angstroms.

The electronics of the setup will drive the scanner in a raster pattern through the sample. The scanner is made out of a piezoelectric material. A piezoelectric material is a polycrystalline ceramic that change dimensions in response to an applied voltage (or vice versa). The strain on the material is ideally linear with the applied voltage:

$$\frac{\Delta l}{l} = dE \tag{7}$$

Here $\Delta l/l$ is the strain ($\mathring{A}/m$), or the variation of length divided by the original length, also called s; d is the strain coefficient ($\mathring{A}/V$) and E is the electric field in V/m.

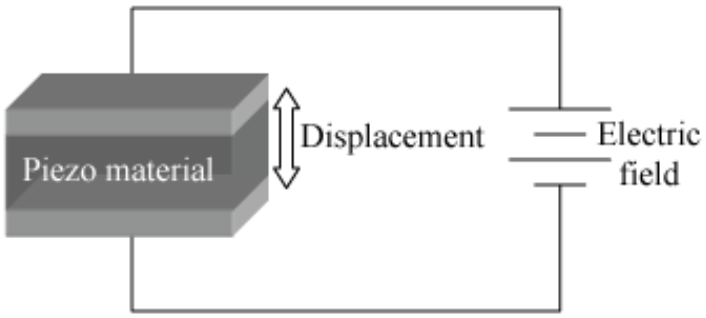

Figure 3. Scheme of the effect on a piezoelectric material that is produced by the application of a voltage or an electric field.

Since it is a polycrystalline material each of this crystals will have its own dipole moment. All these moment are aligned in the construction of the scanner but time and use (or the absence of use) of the device affect this alignment, introducing an error in the measures (because of the change of the response of the material to the potential) due to aging.

Other errors or nonlinearities that must be taken into account are the presence of intrinsic nonlinearities and hysteresis in the material, the delay in the response of it known as creep or the so-called cross coupling due to spurious z-axis component in the x or y-axis movement of the scanner.

With regard to the tip of the cantilever, it is important to point out that the shape of the tip determine the shape resolution of the AFM and can also cause some image artifacts as tip convolution, where the image is determined by the shape of the tip rather than by the shape of the feature studied because the latter is sharper than the former.

With this experimental setup we will perform several measurements during this experiment, such as the surface mapping for samples A and B (Au islands on highly oriented pyrolitic graphite and Au islands on Si respectively). In addition, for sample A we will run two different voltage spectroscopy tasks on a part of the surface that contains both Au and HOPG, as explained in sections 3.1 and 3.2.

3.1 Determination of contact potential between gold and graphite

We will take measurements of the voltage spectra at different locations above the gold islands on graphite by performing a voltage spectroscopy without feedback (i.e. the tip is kept at a constant height). With that data we will be able to estimate the contact potential between Au and HOPG by fitting the voltage spectrum obtained to Equation 4. Here the tip-sample force behaves as a parabola with respect to the effective voltage, which is, as it was already said in section 2.4,

$$V_{eff} = V_{bias} + V_{CPD} \tag{8}$$

The curve resulting of our spectroscopy will be a parabola with its center displaced from zero a certain quantity, which corresponds precisely to this contact potential.

To do this measurement we will obtain the contact potential between tip and sample for both gold and graphite positions, and we will be able then to calculate the contact potential difference between Au and HOPG.

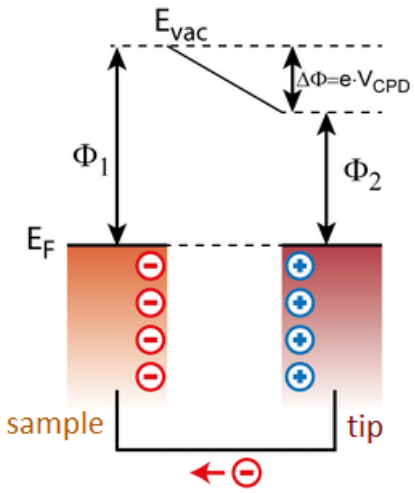

Figure 4. Scheme of the energy bands when tip and sample are in contact[1]. The Fermi energies align and the difference between the work functions of both materials will give us the contact potential.

3.2 Determination of the tip shape

Since the images obtained in atomic force microscopy are the convolution of the topography of the sample and the tip shape of the microscope the characterization of this shape will be of great interest. In order to do so we will perform on different locations of the sample a voltage spectroscopy with feedback, where the tip-sample distance will be controlled by the system and the distance tip-sample will be plotted as a function of the voltage with a constant force gradient.

Here two different simple models for the tip shape will be investigated: a sphere and a cone. From these models two different expressions for the distance as a function of the voltage can be theoretically obtained (Equations 9 and 10). In Figure 5 we can see these theoretical curves for some of the simplest geometries.

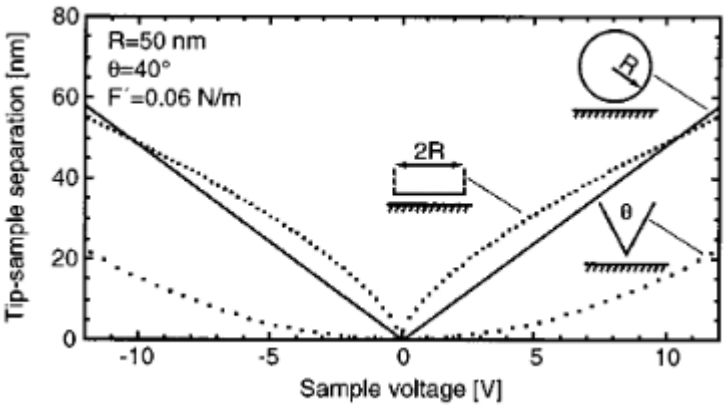

Figure 5. Example of tip-shape separation curves over the voltage for a constant force gradient[6]. We can see how the curves would be if the tip was a sphere, a cone or a plane circular surface.

As we can see for the case of the sphere model the dependence of the tip-sample distance with the voltage is linear (Equation 9) whereas for the cone model it is quadratic (Equation 10). By fitting the experimental data of the spectroscopy with the following theoretical expressions we will decide which model describes best our tip shape and we will also be able to determine the principal parameters of these shapes (radius R for the sphere and cone angle θ):

$$d = \sqrt{\frac{\pi\epsilon_0 R}{F'}}U \tag{9}$$

$$d = \frac{\alpha^2}{4\pi\epsilon_0 F'}U^2 \tag{10}$$

In these equations F' is the force gradient and the parameter α can be derived from the cone angle θ by the following expression:

$$\alpha = \frac{2\pi\epsilon_0}{arcsinh(\frac{1}{tan(\theta/2)})} \tag{11}$$

4 Results

4.1 Resonance frequency

Firstly to initiate the non-contact or dynamic mode of our AFM we determined the resonance frequency at which we needed the cantilever to oscillate. For that task we already had a preset range of frequencies in which we knew the resonance frequency was, so we measured a spectrum of the oscillation amplitude over that frequency range and obtained a curve with a maximum amplitude. That curve is shown in Figure 6.

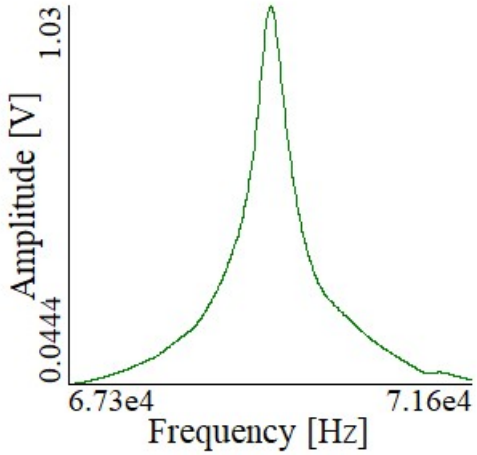

Figure 6: Spectrum of frequencies for the oscillation of the cantilever. The resulting resonance frequency, the center of the peak in the spectrum, is written in Equation 8.

As we can see, we obtained a voltage-frequency spectrum where resonance was reached at a value of the oscillation frequency that was estimated by the computer program as:

$$f_{res} = 69.450kHz \tag{12}$$

4.2 Au on HOPG: Mapping

With all the parameters set for the AFM measurements, we proceeded to obtain several surface images for our first sample of gold islands on a graphite base. Figure 7 shows one of these images where the scan size was set to be 4x4 μm^2

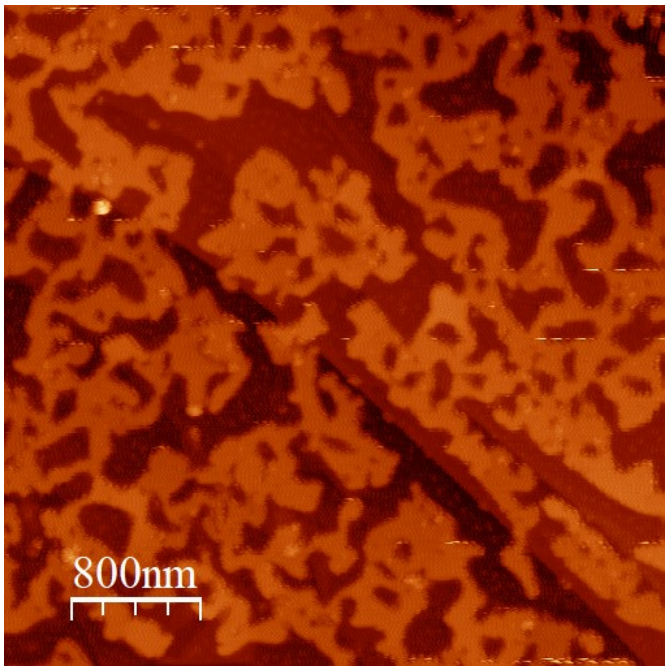

Figure 7: Mapping image of the Au on HOPG surface. The light spots correspond to higher heights, in this case to the Au islands on graphite (dark zones).

Here we can see clearly the structure of our sample: it consists on a layer of gold islands (in our image the light areas, corresponding to higher heights of the topography) on the top of a highly oriented pyrolytic graphite (HOPG) substrate (dark areas in the image).

4.3 Voltage spectroscopy without feedback: contact potential

For the determination of the contact potential difference between the tip and the sample of Au on HoPG we performed several voltage spectroscopies without feedback in twenty different locations of the sample: ten on the gold islands and the other ten on the graphite base. The results of these spectroscopies are shown in Figure 7. As we explained on section 3.1 we can measure the contact potentials for gold and for graphite as the displacement from the center of the spectroscopy curves fitted to parabolas. We performed these fittings on Python.

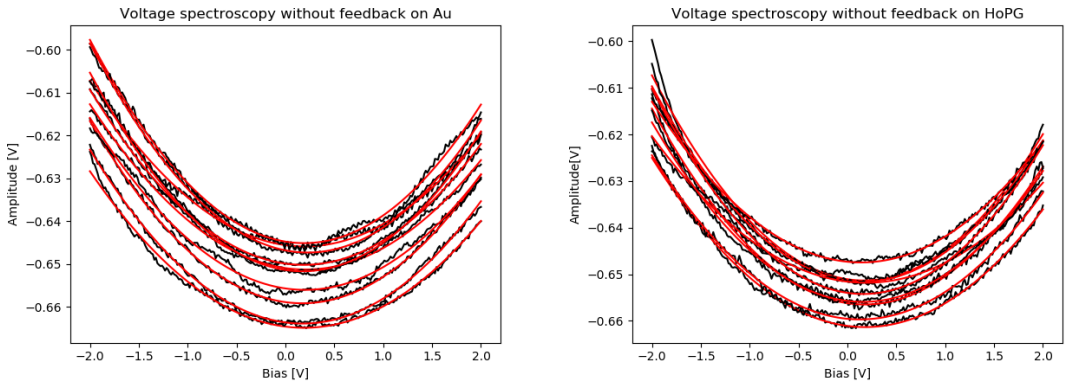

Figure 8: Voltage spectroscopies without feedback for ten different locations on gold (left) and graphite (right) for the same sample of Au on HoPG. The sets of experimental data were fitted with Python to parabolas (solid red curves). All curves have been represented together to show that the displacement is about the same for all locations on the same material.

We got to the following average displacements of the spectroscopy curves for Au and HoPG, i.e., the measured contact potentials for both gold and graphite:

$$V_{tip,Au} = 0.19V \pm 0.02V \tag{13}$$

$$V_{tip,HOPG} = 0.16V \pm 0.02V \tag{14}$$

With these results we can now obtain the work function difference between both materials by simply subtracting one value from the other:

$$\Delta\phi_{HOPG,Au} = (0.03 \pm 0.04)eV \tag{15}$$

4.4 Voltage spectroscopy with feedback: estimation of the tip shape

For the characterization of the tip we performed several spectroscopies with feedback on ten different locations of the surface of our sample and try to fit the experimental data to two different models in order to discern which one of the two describes the better our tip. Figure 9 shows an example of these spectroscopies for one of the locations.

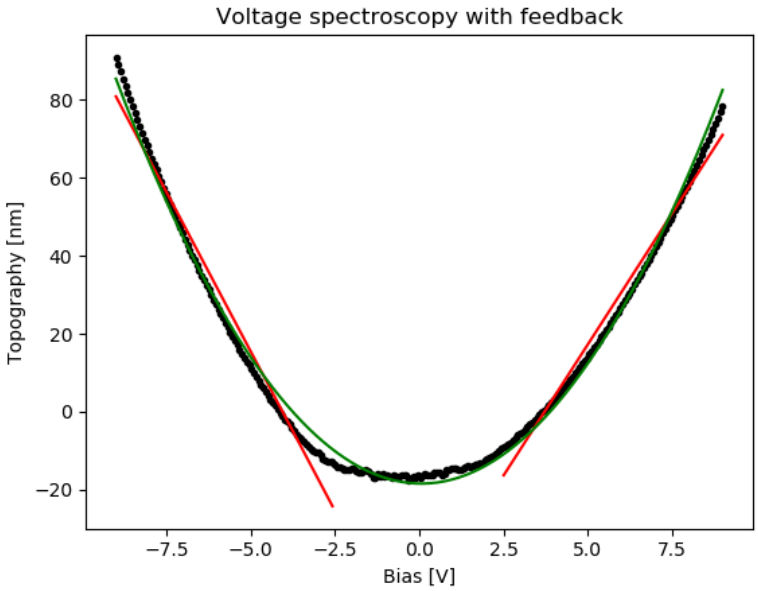

Figure 9: Voltage spectroscopy for a location on a Au on HOPG sample. The experimental data are fit to two linear functions (solid red lines) on their two branches and to a parabola (solid green line), predictions of the tow models we are testing for the tip shape: a sphere and a cone respectively.

As it was exposed on section 3.2 the fitting to the predictions of the two tested models, the spherical tip and the conical tip, also provide us with further information about these shapes. A linear fit was performed in the range of voltages of [-9,-2.5]V and [2.5, 9]V. From this linear fit we can determined a slope which relates to the radius of the sphere through Equation 9. As this slope should be the same for both branches in the ideal case for the shake of symmetry, we averaged in their absolute value the slopes that we obtained for the two branches and we obtained the following slope:

$$\text{m} = 14.7 \pm 1.2 \text{ nm/V}$$

On the other hand, for the quadratic fit we obtained the following mean value for the proportionality factor of the quadratic term:

$$\text{b}= 1.246 \pm 0.006 \text{ nm}/V^2$$

which as we know relates to the angle of the cone through Equation 10. Moreover we have calculated these estimated radius and angle of the cone for our tip using the force gradient derived from Equation 6, knowing that the quality factor of our cantilever was 223.926 ; its spring constant, 2.321 N/m and the ratio of the free amplitude of oscillation and the amplitude of regulation, 1/0.65. Thus we obtained a radius of

$$\text{R} = 90 \pm 2 \text{ nm}$$

for the sphere model and an angle of the cone of

$$\theta = 57.469 \pm 0.003^{\text{o}}.$$

The calculation of these values is rather complex and it is detailed in the Annex.

4.5 Au on Si: Mapping

For our second sample we carried on a mapping of the surface topography adjusting the velocity of scanning in order to obtain the best image as possible avoiding the artifacts due to the nonlinearities of the piezoelectric scanner. Figure 10 shows the topography of our Au on Si sample. Like in Figure 7, the lighter a spot is in the image the higher in height it is on the surface. The scan size was set to be 20x20 μm^2

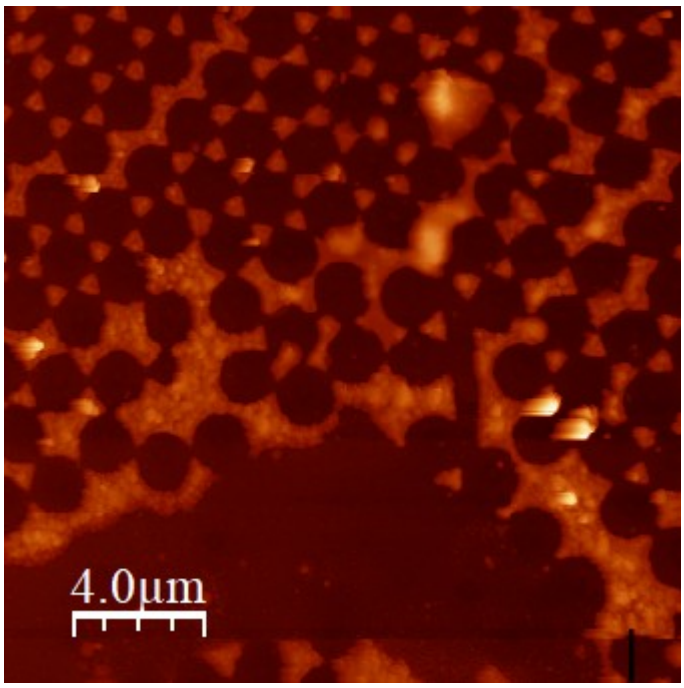

Figure 10: AFM image of the surface for a Au on Si sample, with a scanning velocity of 1 line per second. A pattern of equially spaced circular holes on a gold layer on top of a silicon substrate can be clearly seen on the top right corner of the image (the pattern is mostly destructed on the bottom of the image probably due to the use over the time).

In Figures 11 and 12 we can see the AFM image for the same sample but obtained with different scanner velocities (2 lines per second and 0.5 lines per second respectively). We can observe in them mainly the effect of the delayed response of our feedback system, as for a velocity of 2 lines per second the feedback does not have time to regulate properly. We can also observe differences between the 0.5 lines/s and the 1 line/s ones, as we can see the features on the surface more clearly in Figure 12.

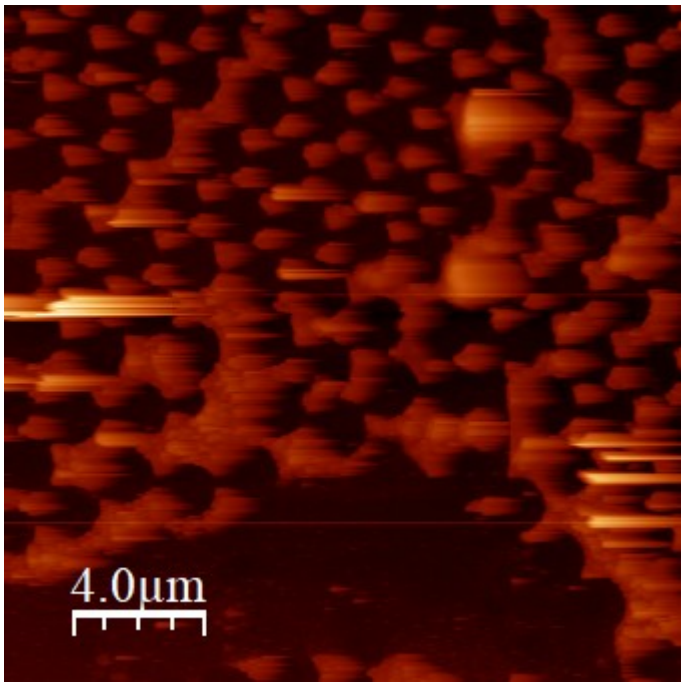

Figure 11: Image of the surface for our B sample with a scanning velocity of 2 lines per second.

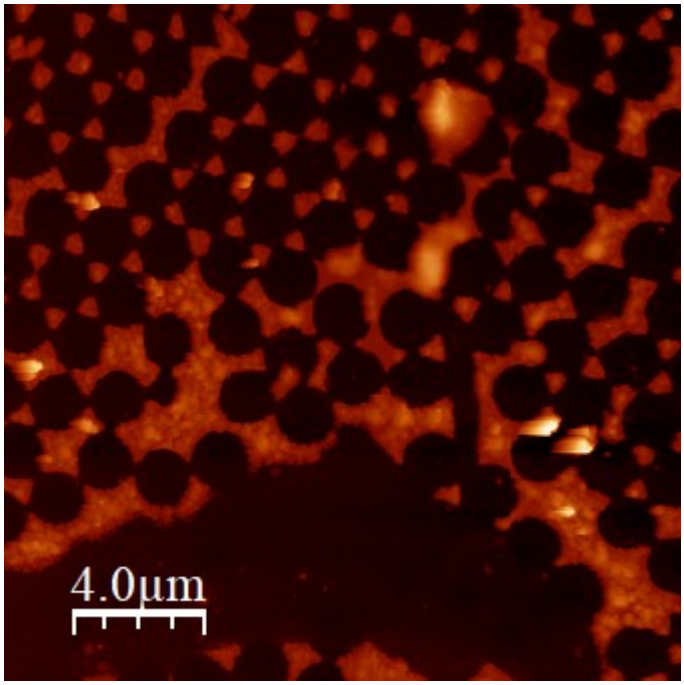

Figure 12: Sample B AFM image for which we established a scanning velocity of 0.5 lines per second.

In Figures 10, 11 and 12 we can see the structure of our sample. The surface shows a layer of gold on a Si(111) substrate where a pattern of equally spaced circular holes was generated through the evaporation of a mask of polystyrene spheres, so we get to see this silicon substrate through the wholes on the gold layer. Moreover we were able to measure the radius of these polystyrene spheres on the image. To do so more accurately we measure the distance for the aligned diameters of several spheres in a row in the three directions of the hexagonal pattern, as they were supposed to have the same size, and calculated the average value by first dividing these distances by the number of spheres taken on each case and then averaging the values for the three dimensions. Distances on the surface image can be measured with the analysis tools of the program WSxM by Nanotec, the same software we have used to display the images of the scanning. In Figure 13 we show how we can calculate from our AFM images the dimensions of the Si circular holes.

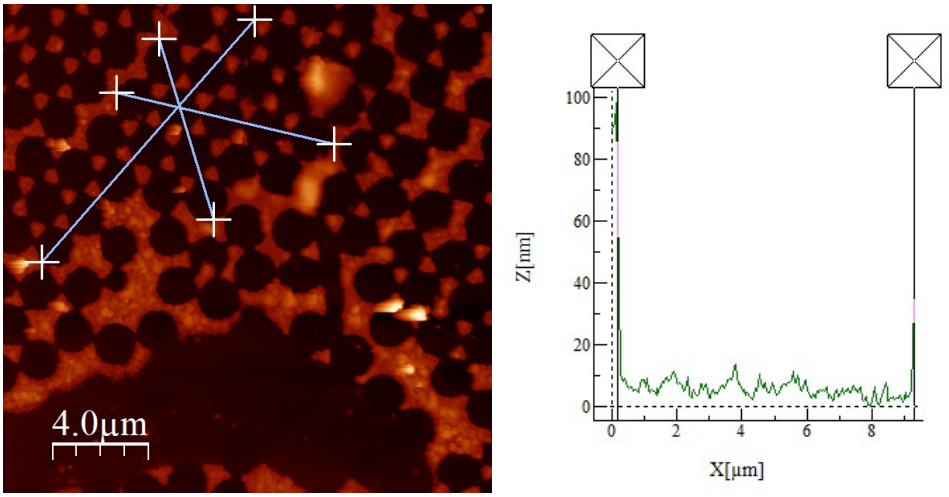

Figure 13: Measurement of the diameter of the whole left by a polystyrene sphere on our sample. In the figure on the right we select a profile by drawing a line on the surface and it is displayed in the figure on the left by the the WSxM software. There we can measure precisely distances in any direction.

The average value for the radius of the polystyrene spheres that we obtained is

$$R_{spheres} = 0.94 \pm 0.3\ \mu$$

5 Discussion

5.1 Scanner nonlinearities

There are several sources of nonlinearities in the piezoelectric scanner, so the potential step that we want to measure does not correspond exactly with the potential step that actually appears in the mapping images. This error may affect of course the results of the spectroscopy experiments as well. We will explain now the most important causes of nonlinearities in our AFM measurements:

- Non linearity. In a real piezoelectric material the change in dimensions is not exactly linear with the electric field.

- Hysteretic behaviour. If we start at a point where the material is held at zero potential energy and we gradually increase the electric field to a final value and then we start to decrease the field to reach the initial point, the material will not follow the same path extension-voltage as it did when we were increasing the potential. This is called hysteresis. It causes errors in the height of the sample features, so at the end of a step it will seem that the intensity of the potential is higher than it actually is.

- Creep. When an abrupt change of the voltage takes place the evolution of the piezoelectric material's dimensions can be divided in two steps: the first one happens in less than a millisecond, but the second one takes a much longer time and is known as "creep". This effect can be minimized if the speed of the tip above the sample is very low, as in this case the scanner would have time to relaxate and we would obtain a more exact image of the surface.

- Aging. It affects the strain coefficient that we talked about in equation 8. This coefficient is not a real constant, but it changes exponentially with time and use of the scanner.

- Cross-coupling. It happens when the scanner, which is supposed to move in the x-y plane, has also a movement component in the z direction. This will cause a deformation in the heights at the sample image that we observe.

Taking into account all these characteristics of a real piezo scanner, the image that we have obtained differs from the ideal one as shown in Figure 14.

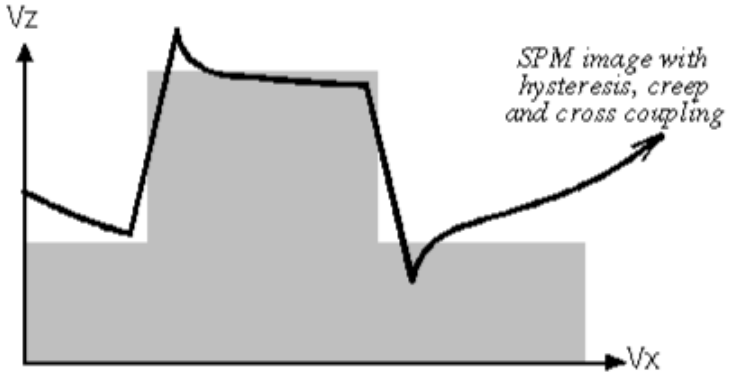

Figure 14: Effect of the nonlinearities of a piezoelectric scanner in the potential curve measured for the AFM microscope. [3]

The effect of all these artifacts could be present during the scanning of our two samples. To correct their effects several measurements were taken for each experiment and then averaged as for the determination of the spheres diameter on the Au on Si sample. Here we also changed the velocity of the scanning to avoid the effect of creep and rotated 90º the plane of the scanning.

5.2 Au on HOPG: contact potential difference

As we already discuss in Section 4.3 we obtained a difference between the work functions of HOPG and Au of:

$$\Delta\phi_{HOPG,Au} = 0.03 \pm 0.04 \text{ eV}$$

The literature values[8][9] for the work functions of Au and HOPG are, respectively,

$$V_{Au}^{lit} = 5.10 - 5.47 \text{ eV}$$

and

$$V_{HOPG}^{lit} = 4.6 \text{ eV}$$

so even taking the lowest value of the range for the gold the literature value for the difference between the work functions would be

$$\Delta\phi_{HOPG,Au}^{lit} = 0.5 \text{ eV}$$

which is far from our experimental results even within its estimated error.

We could blame the pollution of the sample for this difference between our experimental contact potential difference and the corresponding literature value. The presence of a water layer, oxidation on the sample or other impurities that we have seen in the scanning of the surface can heavily influence the work functions of the main compounds of the sample. Moreover, in order to obtain better results from this type of spectroscopy it should be performed in conditions of vacuum or even ultra-high vacuum, so we prevent our sample from adsorbing particles from the air and thus getting contaminated.

5.3 Au on HOPG: tip shape

In Figure 5 we showed some different curves that could be obtained depending on the tip shape. Our real curve can be observed in Figure 9 on the Results section, and from its form we can conclude that the voltage curve corresponds to a spherical tip when the tip-sample separation is big, but tends to look like the conic curve when this separation goes to zero.

From this results we would say that the tip tends to a spherical shape with radius R= 90 ± 2 nm in the part of it that is most far from the sample, but a very sharp conic shape with angle $\theta = 57.468 \pm 0.003°$ for the part of the tip that gets closest to the studied surface. In Figure 15 we present an example of how we think that our tip would look "qualitatively" based on the results that we have obtained in this experiment. If we come to our experimental values for the radius and the angle of the extreme of the tip it would look "quantitatively" different to the one shown in Figure 15, for the conical part would be much blunter and the spherical basis much bigger compared to the cone.

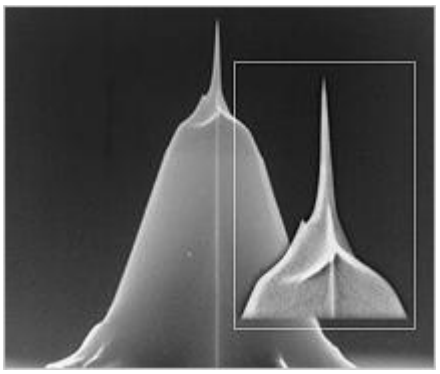

Figure 15: Example of a tip image[10] that has a conic shape in the part that is closest to the surface and something close to a spherical behaviour as we go far away from the sample. For our measured values the conical part of the tip would look considerably less sharp and the spherical part would be much bigger in relation to the cone as it is in the figure.

6 Conclusions

We obtained images of two different samples, (a surface gold islands on a HOPG substrate and a layer of gold on a silicon substrate with a pattern of equally spaced circular gaps) by means of atomic force microscopy. It helped us not only to characterize the samples but also to better understand this microscopy technique.

We also performed two different spectroscopy experiments on the surface of the first sample. This additional experiments allowed us to study in more depth the surface structure, such as the dimensions of the Si spheres or the contact potential between Au and HOPG. We also could estimate the shape of the tip used in this AFM experience.

References

[1] Christian Lotze, Fundamental Processes in Single Molecule Junctions: Interplay of Forces and Electronic Effects, https://www.researchgate.net/

[2] Sascha Sadewasser, Christian Lotze; Manual: Atomic Force Microscope

[3] ThermoMicroscopes, Basic guide to Scanning Probe Microscopy

[4] Nanotec Electronica s.l. “SPM user manual”, www.nanotec.es

[5] Lü et al.Appl. Phys. A 66, 273 (1998)

[6] Olssen et al., J. Appl. Phys. 84, 8, 4060 (1998)

[7] Martin et al., J. Appl. Phys. 61, 10, 4723 (1987)

[8] Wikipedia, https://en.wikipedia.org/wiki/Work-function

[9] http://rsl.eng.usf.edu/Documents/Tutorials/TutorialsWorkFunction.pdf

[10] https://www.nanoandmore.com/AFM-Probe-NW-AR5-NCHR

7 Annex: Calculation of the parameters of the shape of the tip

In Table 1 we can see the values of the parameters of the cantilever that we used in the calculations of the radius of the tip in the sphere model and of its angle in the conical model. The constant force gradient was obtained through equation 6.

Quality factor Q	223.926
Spring constant k [N/m]	2.321
Ratio a	1.538
Force gradient F' [N/m]	0.012

Table 1: Parameters of the cantilever used in the voltage spectroscopy with feedback for the estimation of the tip shape

From equation 9 and knowing the slope of the linear fitting of the distance d as a function of the voltage one can easily derive the expression of the radius and its error:

$$R = \frac{m^2 F'}{\pi \epsilon_0} \tag{16}$$

$$\Delta R = \frac{2mF'}{\pi \epsilon_0} \Delta m \tag{17}$$

where we have used the value of the universal constant $\epsilon_0 = 8.854 \cdot 10^{-12} \frac{C^2}{Nm}$.
Analogously one can derive the expression for the angle θ and its error in the cone model from equations 10 and 11, knowing the prefactor b in the fit to a parabola of the experimental data:

$$\theta = 2 \cdot \arctan \frac{1}{\sinh \sqrt{\frac{2\pi\epsilon_0}{F'b}}} \tag{18}$$

$$\Delta\theta = \left| \frac{\sqrt{\frac{\pi\epsilon_0}{F'b}} \coth \sqrt{\frac{\pi\epsilon_0}{F'b}} \operatorname{csch} \sqrt{\frac{\pi\epsilon_0}{F'b}}}{b \cdot \operatorname{csch}^2 \sqrt{\frac{\pi\epsilon_0}{F'b}} + b} \right| \Delta b \tag{19}$$